Acta Cryst. (1996). B52, 16–31

The Compositional Dependence of Octahedral Tilting in Orthorhombic and Tetragonal Perovskites

NOEL W. THOMAS

School of Materials, University of Leeds, Leeds LS2 9JT, England

(*Received 6 August 1994; accepted 10 May 1995*)

Abstract

A new parameterization is defined for the quantitative description of octahedral tilting in orthorhombic and tetragonal perovskites. It contains six parameters, s_1, s_2, s_3, θ_x, θ_y and θ_z. s_1, s_2 and s_3 refer to the lengths of the lines or 'stalks' joining pairs of opposite octahedral vertices, and θ_x, θ_y and θ_z to the angles subtended by these stalks with pseudo-cubic axes x, y and z. An equation is derived for the dependence of polyhedral volume ratio, V_A/V_B, on these parameters: $V_A/V_B = 6\cos^2\theta_m\cos\theta_z - 1$, where $\theta_m = (\theta_x + \theta_y)/2$. To a good approximation, lengths s_1, s_2 and s_3 do not affect V_A/V_B. The validity of this equation is tested by reference to the known crystal structures of 48 ternary oxide and fluoride perovskites, and its versatility demonstrated by application to the structures of some ternary palladium and platinum hydrides. The relationship of the approach to Glazer's system of nomenclature for octahedral tilting in perovskites is considered, in particular concerning the numbers of tilts operative in a given structure. A comparison is also made with the parameterization proposed for octahedral tilting and distortion in rhombohedral perovskites [Thomas & Beitollahi (1994). *Acta Cryst.* B50, 549–560]. Factors governing the choice of rhombohedral or orthorhombic symmetry are discussed, with the significance of rhombohedral symmetry in obtaining ferroelectric properties brought out. Through the compilation of a table of AO_{12} and BO_6 polyhedral volumes, the prospect is identified of predicting both the degree of octahedral tilting and the likelihood of ferroelectric behaviour for novel, hypothetical oxide compositions.

1. Introduction

Perovskites are of widespread interest, not least because of their diverse physical and chemical properties. Moreover, a quantitative study of their crystal structures is particularly relevant to physical properties such as ferroelectricity, antiferroelectricity, piezoelectricity and optical activity, since these are fundamentally due to the dipole moments caused by ionic displacements. Earlier work (Thomas, 1989) has shown that the structures of perovskites (ABX_3) may be meaningfully analysed in terms of the volumes of the AX_{12} and BX_6 cation coordination polyhedra, thereby giving insight into the compositional dependence of their crystal structures. The approach provides a framework for relating *chemical composition* with *physical properties*, where the *mechanism* of the relationship can be analysed in terms of the crystal structure. This capability is an important contribution to the *chemical design* of perovskites for particular desirable physical applications.

In essence, the perovskite structure consists of a three-dimensionally linked network of BX_6 octahedra, with A ions forming AX_{12} cuboctahedra to fill the spaces between the octahedra. In view of these inviolable topological and geometrical constraints, there are only three structural degrees of freedom:

(*a*) displacement of cations A and B from the centres of their cation coordination polyhedra, AX_{12} and BX_6;

(*b*) distortions of the anionic polyhedra coordinating A and B ions;

(*c*) tilting of the BX_6 octahedra about one, two or three axes.

In *ferroelectric* phases of rhombohedral symmetry, displacements (*a*) and distortions (*b*) are correlated, so that relatively larger B ions can be stabilized at an off-centre position. Potential energy calculations reveal also that parallel A- and B-ion displacements, along the trigonal axis, are more favourable than anti-parallel displacements. In addition, any tilting of octahedra (*c*) in rhombohedral perovskites (whether ferroelectric or not) can be described by a single tilt angle about the trigonal axis (Thomas & Beitollahi, 1994). *Orthorhombic* perovskites, by comparison, present a wider range of polyhedral distortions and tilting possibilities, which form the subject matter of this article. As well as orthorhombic perovskites, tetragonal perovskites with octahedral tilting are also considered, since the definition of tilt angles is identical in both cases.

The treatment and discussion of octahedral tilting in perovskites was initiated by Megaw (1966, 1969) and developed by Glazer (1972, 1975). The latter work demonstrated that the space group was largely determined by the pattern of octahedral tilting. Furthermore, a classification of octahedral tilting in terms of ten alternative tilt systems was proposed. Regular BX_6 octahedra were assumed, with all tilts considered as

combinations of component tilts about the three pseudo-cubic axes. Since the atomic coordinates in the final tilt arrangement depended on the order in which the component tilt operations were carried out, the approach was intended for a description of structures, rather than their quantitative derivation (Glazer, 1972). The definition of tilt angles employed here differs from Glazer's, since the objective is to formulate a *quantitative* relationship between tilting and polyhedral volume ratio.

The strength of Glazer's parameterization lies in the ease with which an evaluation of the numbers and directions of tilts may be carried out. It is intended that the alternative definition of tilt angles used here is sufficient to calculate the polyhedral volume ratio, V_A/V_B, but not to regenerate the coordinates of all ions unambiguously. This capability would require additional information about the axes of rotation, which would be too cumbersome to be quoted routinely. The parameterization to be developed here can also take octahedral irregularities into account, as the values of the tilt angles are derived by computational analysis of experimental structural data.

In articulating the quantitative relationship between octahedral tilt angles and V_A/V_B, the dependence of the various manifestations of octahedral tilting on chemical composition can be understood. The quantitative framework thus developed is sufficiently general to be applied to all perovskites in which tilting occurs. This generality is demonstrated by applying the analysis not merely to metal oxides and fluorides, but also to some novel ternary platinum and palladium hydrides, which have been found to crystallize with tilted perovskite structures.

2. Method

2.1. *Derivation of the relationship between V_A/V_B and octahedral tilt angles*

The polyhedral volume ratio, V_A/V_B, is obtained by dividing the volume of the AX_{12} cation coordination polyhedron by that of the BX_6 coordination polyhedron. Further, a feature of perovskites is that these polyhedra fill space (Thomas, 1989), such that

$$V_u = Z(V_A + V_B). \tag{1}$$

It follows that the ratio V_A/V_B can be derived by calculating the unit-cell volume V_u and the octahedral volume V_B.

The parameterization requires six parameters (Fig. 1): s_1, s_2, s_3: separations of three pairs of opposite octahedral vertices (lengths of three 'octahedral stalks'); θ_x, θ_y, θ_z: tilt angles, defined as angles between octahedral stalks and pseudo-cubic axes x, y and z. The structures of all perovskites, regardless of their symmetry, may be referred to a pseudocubic cell ($a_p \approx b_p \approx c_p$, $\alpha \approx \beta \approx \gamma \approx 90°$), whose axes are oriented closest to the lines joining opposite octahedral vertices (stalks). Fig. 1 is a schematic representation of a typical tilted structure. It shows a projection of a three-dimensional tilt system in the xy plane, referred to pseudo-cubic axes. The relevant pseudo-cubic cell is drawn as a solid line. θ_x and θ_y are the two angles subtended by the two octahedral 'stalks' lying close to or in the xy plane with the x and y axes, *i.e.* θ_x corresponds to $\angle ABC$ and θ_y to $\angle DEF$. The + and − signs denote schematically the z heights of octahedral vertices, either above (+) or below (−) the xy plane, according to a possible tilt system. This particular system is consistent with a smaller unit cell of orthorhombic symmetry, delineated with dashed lines. s_1 and s_2 represent the lengths of the two octahedral stalks lying close to the xy plane, with s_3 (not shown) referring to the stalk closest in orientation to the plane-normal, *i.e.* the pseudo-cubic z axis. Whenever $s_1 \neq s_2$, $\theta_x \neq \theta_y$.

It is assumed for the derivation of the relationship between V_A/V_B and tilt angles θ_x, θ_y and θ_z that the three octahedral stalks intersect at right angles. In general, this is only a small approximation. Given this assumption, inspection of Fig. 1 reveals that the angles between the x and y axes of the pseudo-cubic cell are $90° \pm (\theta_y - \theta_x)$, with the area of the cell face in the xy plane equal to $a_{pc}b_{pc}\sin(\pi/2-(\theta_y - \theta_x)) = a_{pc}b_{pc}\cos(\theta_y - \theta_x)$. Inspection of Fig. 1 reveals that

$$a_{pc} = b_{pc} = s_1 \cos\theta_x + s_2 \cos\theta_y. \tag{2}$$

Since all the octahedral stalks subtending smallest angles with the z axis have length s_3, the z axis is unique in this parameterization. This is to be compared with the x and y axes, along which the stalks subtending smallest angles alternate between lengths s_1 and s_2. Thus

$$c_{pc} = 2s_3 \cos\theta_z. \tag{3}$$

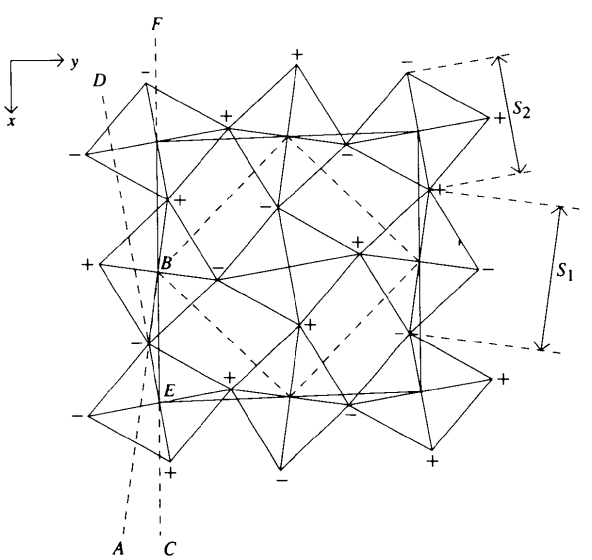

Fig. 1. Definition of parameters s_1, s_2, θ_x and θ_y used to quantify octahedral tilting.

It follows that the pseudo-cubic cell constructed as above contains eight whole octahedra, *i.e.* $Z_{pc} = 8$. In cases where $\theta_z = 0$, the c cell parameter is equal to $c_{pc}/2$, *i.e.* $Z_{pc} = 4$. Other cases, where $Z_{pc} = 16$, or where $a_{pc} \neq b_{pc}$, are a consequence of either different tilt systems or of particular patterns of cation displacement. For the general development of the argument, however, it is assumed that Z_{pc} is equal to 8.

The volume of the pseudo-cubic cell is given by

$$V_u = 2(s_1 \cos\theta_x + s_2 \cos\theta_y)^2 s_3 \cos\theta_z \cos(\theta_y - \theta_x). \quad (4)$$

Thus, the polyhedral volume ratio $V_A/V_B = \frac{1}{8}(V_u - 8V_B)/V_B = V_u/8V_B - 1$. As the three octahedral stalks are regarded as perpendicular to one another, $V_B = s_1 s_2 s_3/6$ and

$$V_A/V_B = (3/2)[(s_1 \cos\theta_x + s_2 \cos\theta_y)^2/s_1 s_2] \times \cos\theta_z \cos(\theta_y - \theta_x) - 1. \quad (5)$$

Since θ_x and θ_y differ only slightly as a result of unequal s_1 and s_2 values, θ_x may be written as $\theta_m - \Delta$ and θ_y as $\theta_m + \Delta$, where θ_m is the mean of θ_x and θ_y and Δ is a very small angle. This permits a re-expression of the $s_1 \cos\theta_x + s_2 \cos\theta_y$ term in (5) as

$$(s_1 + s_2)\cos\theta_m \cos\Delta + (s_1 - s_2)\sin\theta_m \sin\Delta. \quad (6)$$

Since the second of these two terms is a product of three factors, two of which are very small, *i.e.* $s_1 - s_2$ and $\sin\Delta$, it is considerably smaller than the first term and may be disregarded. It is also a very good approximation to write $\cos\Delta = 1$. (5) can thus be simplified as

$$V_A/V_B = (3/2)[(s_1 + s_2)^2/s_1 s_2]\cos^2\theta_m \cos\theta_z \cos 2\Delta - 1. \quad (7)$$

Since the difference between s_1 and s_2 is generally not very large, the dependence of the V_A/V_B ratio on the stalk lengths is weak, since $(s_1 + s_2)^2/s_1 s_2 \simeq 4$. Writing $(s_1 + s_2)^2/s_1 s_2$ as equal to 4 and $\cos 2\Delta$ equal to 1 (*i.e.* disregarding deviations of γ_{pc} from 90°), it follows that

$$V_A/V_B = 6\cos^2\theta_m \cos\theta_z - 1. \quad (8)$$

Thus, the polyhedral volume ratio V_A/V_B is determined largely by the average of tilt angles θ_x and θ_y in the xy plane, θ_m, and the angle subtended by the octahedral axes of length s_3 with the z axis, θ_z. The prediction is that the polyhedral volume ratio V_A/V_B has the value 5 in the absence of tilting, falling to lower values in structures with tilted octahedra.

3. Examination of experimentally determined structures

Structures to be examined fall into two categories: (i) metal oxides and fluorides and (ii) hydrides of platinum or palladium with alkali ions. Although the former compounds are more prevalent as perovskites, the second category is included to demonstrate the versatility of the methodology.

(i) *Metal oxides and fluorides*

Table 1 gives the space groups, temperatures and derived pseudo-cubic cell constants for 48 orthorhombic and tetragonal oxides and fluorides, with structures retrieved from the Inorganic Crystal Structure Database (ICSD). Data for the final structure, $PbZrO_3$, were taken from a recent publication by Glazer, Roleder & Dec (1993). Atomic coordinates and pseudo-cubic cell constants were generated computationally in a four-stage procedure: (i) resetting, where necessary, of unit-cell axes as given in the ICSD into the standard setting; (ii) generation, from the symmetry operations of the relevant space group, of all the atomic coordinates within the orthorhombic or tetragonal unit cell; (iii) generation of atomic coordinates of nearest-neighbour translationally related unit cells and identification of the appropriate pseudo-cubic cell from these; (iv) calculation of pseudo-cubic lattice parameters and re-expression of atomic coordinates in terms of these.

In all cases, apart from space group 63 (*Cmcm*), $a_{pc} = b_{pc}$ and in all cases, $\alpha_{pc} = \beta_{pc} = 90°$. Except for the two $PbZrO_3$ structures, a_{pc} is of the order 8 Å, indicating that the pseudo-cubic cell corresponds to 2×2 octahedra in the xy plane, as shown in Fig. 1. Cells with $Z_{pc} = 4$ are associated with structures in which $\theta_z = 0$. Since most structures have Z_{pc} values of 8, they are characterized by non-zero values of θ_x, θ_y and θ_z. Values of Z_{pc} greater than 8 are to be found in the $PbZrO_3$ structures and in the room-temperature structure of $NaNbO_3$. In the former, structures with 4×4 octahedra in the xy plane are found, together with a non-zero θ_z value. The doubling of the a_{pc} axis is due to cationic displacements, rather than to the adoption of a complex octahedral tilting system. In the latter, a doubling of the c_{pc} axis is observed, corresponding to the adoption of a complex tilt system.

Examination of Table 1 reveals that the commonest space group is no. 62 (*Pnma*). For this reason, stalk lengths, tilt angles and polyhedral volumes for structures in this space group are listed separately from other structures, in Table 2. In Table 2, s_1, s_2 and s_3 correspond to octahedral stalk lengths as defined in equations (2) and (3). The factor $(s_1 + s_2)^2/s_1 s_2$ is equal to 4.000 in all structures, apart from three, $NaTaO_3$ (ICSD No. 9090), $GdFeO_3$ and $NaZnF_3$, indicating that the approximation made in proceeding from equation (7) to (8) is a good one. In the first of these structures, the TaO_6 octahedra are extremely distorted, to an extent not found in any other structure. For all structures, θ_m and θ_z values can be substituted into (8) to obtain the *theoretical* polyhedral volume ratio $[V_A/V_B]^t$. This is to be compared with the *actual* polyhedral volume ratio, $[V_A/V_B]^a$, which is

Table 1. *Compositions, ICSD codes, temperatures, space groups and derived pseudo-cubic cell parameters for all oxides and fluorides analysed*

Composition	ICSD no.	Temperature (K)*	Space group	Z_{pc}	a_{pc} (Å)	b_{pc} (Å)	c_{pc} (Å)	γ_{pc} (°)	Ref.
$SrZrO_3$	500		62	8	8.2032		8.196	87.7136	(1)
$SrZrO_3$	1185	1175	140	8	8.2732		8.295	90.0001	(2)
$SrZrO_3$	1186	1035	63	8	8.2530	8.2660	8.271	90.0000	(2)
$BaCeO_3$	2237		62	8	8.8014		8.781	89.7883	(3)
$BaPrO_3$	2239		62	8	8.7646		8.722	89.6949	(3)
$KMnF_3$	2471		127	8	8.3354		8.348	90.0000	(4)
$YAlO_3$	2526		62	8	7.4325		7.375	88.3647	(5)
$KNbO_3$	3838		38	4	8.0688		3.971	89.7289	(6)
$SmAlO_3$	4597		62	8	7.4819		7.474	90.0108	(7)
$NaNbO_3$	8460	773	59	8	7.8610		7.856	90.0000	(8)
$NaNbO_3$	8461	803	63	8	7.8550	7.8642	7.870	90.0000	(8)
$NaTaO_3$	9090		62	8	7.7818		7.795	90.3853	(9)
$NaTaO_3$	9091	803	63	8	7.8450	7.8540	7.863	90.0000	(9)
$NaTaO_3$	9092	873	63	8	7.8560	7.8720	7.860	90.0000	(9)
$NaTaO_3$	9093	893	127	4	7.8560		3.934	90.0000	(9)
$NaNbO_3$	9014		57	16	7.8292		15.520	90.6210	(10)
$NaNbO_3$	9094	813	63	8	7.8590	7.8660	7.877	90.0000	(9)
$NaNbO_3$	9325	873	127	4	7.8687		3.943	90.0000	(11)
$HoNiO_3$	10621		62	8	7.5633		7.425	86.4747	(12)
$PrFeO_3$	12457		62	8	7.8209		7.786	89.0054	(13)
$NdFeO_3$	12458		62	8	7.8049		7.768	88.6400	(13)
$SmFeO_3$	12459		62	8	7.7773		7.711	87.9474	(13)
$EuFeO_3$	12460		62	8	7.7644		7.685	87.5580	(13)
$TbFeO_3$	12462		62	8	7.7297		7.635	87.1065	(13)
$DyFeO_3$	12463		62	8	7.7103		7.623	86.8889	(13)
$HoFeO_3$	12464		62	8	7.6887		7.602	86.7010	(13)
$ErFeO_3$	12465		62	8	7.6719		7.591	86.6303	(13)
$TmFeO_3$	12466		62	8	7.6593		7.584	86.5613	(13)
$YbFeO_3$	12467		62	8	7.6331		7.570	86.5601	(13)
$LuFeO_3$	12468		62	8	7.6121		7.565	86.4441	(13)
$LaFeO_3$	13344		62	8	7.8602		7.867	89.8969	(14)
$PbZrO_3$	15284		32	32	16.6425		8.220	90.0000	(15)
$BaTiO_3$	15285	263	38	4	8.0264		3.990	90.1313	(16)
$KMnF_3$	15943	95	62	8	8.3227		8.376	90.0000	(17)
$KMnF_3$	15944	65	62	8	8.3439		8.330	90.0000	(17)
$KMnF_3$	15945	84	62	8	8.3227		8.376	90.0000	(17)
$GdFeO_3$	25957		62	8	7.7537		7.668	90.0000	(18)
$CaTiO_3$	26633		62	8	7.6524		7.640	89.3435	(19)
$CdTiO_3$	26634		62	8	7.5856		7.618	88.7502	(20)
$CdTiO_3$	26635		33	8	7.5856		7.618	88.7502	(20)
$PrFeO_3$	27876		62	8	7.8330		7.783	88.9138	(21)
$KCuF_3$	31453		140	8	8.2831		7.849	90.0000	(22)
$SmNiO_3$	34154		62	8	7.6124		7.568	88.8400	(23)
$NaMgF_3$	36355		62	8	7.6439		7.654	88.3145	(24)
$NaNiF_3$	36356		62	8	7.7055		7.695	88.2754	(24)
$NaZnF_3$	36357		62	8	7.7706		7.765	88.2273	(24)
$NaCoF_3$	36358		62	8	7.7991		7.786	88.0882	(24)
$PbZrO_3$			55	32	16.6609		8.226	89.9708	(25)

References (in CODEN form): (1) ACBCA 32 3243 1976; (2) ACBCA 34 752 1978; (3) ACBCA 28 956 1972; (4) JUPSA 39 100 1975; (5) MRBUA 10 85 1975; (6) JPSOA 6 2559 1973; (7) JSSCB 4 11 1972; (8) PHMA8 26 995 1972; (9) ACBCA 36 1007 1980; (10) ACBCA 25 861 1969; (11) PHMA8 25 1119 1972; (12) JSSCB 3 582 1971; (13) ACBCA 26 2008 1970; (14) MRBUA 6 23 1971; (15) PHRVA 105 849 1957; (16) PHRVA 105 856 1957; (17) PHRVA 121 376 1961; (18) ZNBAD 41 1391 1986; (19) ACSCE 43 1668 1987; (20) ACSCE 43 1668 1987; (21) MRBUA 111 109 1985; (22) ASBSD 46 131 1990; (23) JSSCB 91 225 1991; (24) ZAACA 616 133 1992; (25) Glazer, Roleder & Dec (1993). *Room temperature, except where explicitly stated otherwise.

obtained by dividing V_A by V_B. V_A and V_B are calculated computationally, using the methodology defined in an earlier paper (Thomas, 1991*a*). Agreement between $[V_A/V_B]^a$ and $[V_A/V_B]^t$ is generally very good, with most discrepancies, $\Delta[V_A/V_B] = [V_A/V_B]^t - [V_A/V_B]^a$, less than ± 0.003. The main source of discrepancy lies in the approximation in the derivation of (8) that the three octahedral stalks, of lengths s_1, s_2 and s_3, intersect at right angles. This constraint is not imposed by *Pnma* symmetry, however, where small deviations from normal intersection frequently occur. The deviation from perpendicular intersection is quantified by the parameter $\Delta_{perp} = 1 - \sin\alpha_{xy} \sin\alpha_{yz} \sin\alpha_{zx}$, as given in the right-hand column of Table 2. α_{xy} represents the angle between the octahedral stalk of orientation closest to that of the x axis and the stalk oriented closest to the y axis *etc.* Thus, for perpendicular intersection of all three stalks, this parameter is equal to zero.

The largest discrepancy is found in the structure $NaTaO_3$ (ICSD No. 9090), where $\Delta[V_A/V_B] = -0.478$, and in which the factor $(s_1+s_2)^2/s_1s_2$ also shows its largest deviation from 4. It is not immediately apparent why the room-temperature phase of $NaTaO_3$ should have such distorted octahedra, particularly as the associated

Table 2. *Octahedral stalk lengths, tilt angles, polyhedral volumes and ratios, values of Δ_{perp} for oxides and fluorides in space group 62*

Composition	ICSD no.	s_1 (Å)	s_2 (Å)	s_3 (Å)	$(s_1+s_2)^2/s_1s_2$	θ_m (°)	θ_t (°)	V_A (Å^3)	V_B (Å^3)	$[V_A/V_B]^a$	$[V_A/V_B]^i$	$\Delta[V_A/V_B]$	Δ_{perp}
$SrZrO_3$	500	4.1671	4.1886	4.1894	4.000	10.963	11.990	56.7586	12.1812	4.660	4.657	−0.003	4.733×10^{-4}
$BaCeO_3$	2237	4.4464	4.5189	4.4812	4.000	10.973	11.545	70.0310	14.9950	4.670	4.666	−0.004	7.680×10^{-4}
$BaPrO_3$	2239	4.4429	4.4468	4.4547	4.000	9.623	11.773	69.0935	14.6568	4.714	4.710	−0.004	7.839×10^{-4}
$YAlO_3$	2526	3.8210	3.8416	3.8030	4.000	14.077	14.155	41.6046	9.3002	4.474	4.474	0.000	3.667×10^{-4}
$SmAlO_3$	4597	3.7927	3.7984	3.8000	4.000	9.731	10.449	43.1760	9.1222	4.733	4.732	−0.001	1.955×10^{-4}
$NaTaO_3$	9090	3.3845	4.4525	3.9583	4.076	6.871	10.052	49.6379	9.3647	5.301	4.823	−0.478	5.747×10^{-2}
$HoNiO_3$	10621	3.8727	3.9173	3.8385	4.000	13.858	14.722	43.3104	9.6806	4.474	4.470	−0.004	2.610×10^{-3}
$PrFeO_3$	12457	4.0171	4.0303	4.0017	4.000	13.627	13.386	48.7268	10.7946	4.514	4.513	−0.001	3.291×10^{-4}
$NdFeO_3$	12458	4.0206	4.0342	4.0088	4.000	14.310	14.335	48.2999	10.8332	4.459	4.458	−0.001	3.656×10^{-4}
$SmFeO_3$	12459	4.0137	4.0607	4.0020	4.000	15.590	15.553	47.3984	10.8655	4.362	4.363	+0.001	5.068×10^{-4}
$EuFeO_3$	12460	4.0190	4.0590	3.9997	4.000	16.018	16.117	46.9919	10.8673	4.324	4.325	+0.001	6.668×10^{-4}
$TbFeO_3$	12462	4.0152	4.0600	3.9939	4.000	16.820	17.094	46.1086	10.8414	4.253	4.255	+0.002	9.149×10^{-4}
$DyFeO_3$	12463	4.0087	4.0672	3.9960	4.000	17.307	17.480	45.7158	10.8481	4.214	4.216	+0.002	9.789×10^{-4}
$HoFeO_3$	12464	4.0016	4.0616	3.9961	4.000	17.531	17.979	45.2699	10.8125	4.187	4.189	+0.002	1.143×10^{-3}
$ErFeO_3$	12465	4.0039	4.0573	4.0055	4.000	17.879	18.633	44.9196	10.8326	4.147	4.150	+0.003	1.124×10^{-3}
$TmFeO_3$	12466	4.0049	4.0529	4.0093	4.000	18.095	18.951	44.6842	10.8298	4.126	4.127	+0.001	1.519×10^{-3}
$YbFeO_3$	12467	4.0015	4.0514	4.0110	4.000	18.581	19.324	44.2137	10.8198	4.086	4.087	+0.001	1.625×10^{-3}
$LuFeO_3$	12468	3.9945	4.0479	4.0164	4.000	18.827	19.651	43.8809	10.8074	4.060	4.062	+0.002	1.511×10^{-3}
$LaFeO_3$	13344	4.0033	4.0143	4.0188	4.000	11.373	11.827	49.9954	10.7601	4.646	4.644	−0.002	3.694×10^{-4}
$KMnF_3$	15943	4.2001	4.2001	4.1984	4.000	7.794	4.032	60.2838	12.2382	4.926	4.875	−0.051	8.678×10^{-3}
$KMnF_3$	15944	4.2315	4.2315	4.1854	4.000	9.624	5.663	60.0329	12.4589	4.818	4.804	−0.014	2.542×10^{-3}
$KMnF_3$	15945	4.1830	4.1830	4.2135	4.000	5.833	6.302	60.2376	12.2845	4.904	4.902	−0.002	2.369×10^{-4}
$GdFeO_3$	25957	3.8990	4.1602	4.0162	4.004	15.835	17.325	46.7173	10.8371	4.311	4.301	−0.010	1.879×10^{-3}
$CaTiO_3$	26633	3.9101	3.9175	3.9005	4.000	12.141	11.659	45.9648	9.9560	4.617	4.616	−0.001	1.573×10^{-4}
$CdTiO_3$	26634	3.9271	3.9301	3.9389	4.000	15.107	14.758	44.6537	10.1268	4.409	4.408	−0.001	5.062×10^{-4}
$PrFeO_3$	27876	4.0203	4.0463	4.0108	4.000	13.822	14.011	48.8090	10.8715	4.490	4.489	−0.001	2.363×10^{-4}
$SmNiO_3$	34154	3.8865	3.9230	3.9226	4.000	12.902	15.178	44.8463	9.9617	4.502	4.502	0.000	6.323×10^{-4}
$NaMgF_3$	36355	3.9477	3.9508	3.9527	4.000	14.584	14.489	45.6088	10.2698	4.441	4.441	0.000	4.747×10^{-4}
$NaNiF_3$	36356	4.0052	4.0104	4.0028	4.000	15.989	16.014	46.3765	10.7088	4.331	4.330	−0.001	6.549×10^{-4}
$NaZnF_3$	36357	3.9952	4.0942	4.0507	4.001	16.140	16.567	47.5520	11.0290	4.312	4.307	−0.005	1.234×10^{-3}
$NaCoF_3$	36358	4.0713	4.0758	4.0785	4.000	16.808	17.347	47.8990	11.2668	4.251	4.248	−0.003	1.137×10^{-3}

octahedral volume, V_B, at 9.3647 Å^3, is significantly smaller than values for the three higher temperature structures (see Table 4).

In focusing on octahedral tilts and polyhedral volumes, only the positions of the anions (O^{2-} or F^-) are being taken into account. A full treatment of the structures also requires a consideration of the positions of the *A* and *B* cations within their coordination polyhedra, particularly as cationic displacements have a significant influence on physical properties such as ferroelectricity and antiferroelectricity. Such information is presented in Table 3, where use is made of the quantities quadratic elongation (QE) and bond angle variance (BAV). As introduced by Robinson, Gibbs & Ribbe (1971) and applied previously to perovskites (Thomas, 1989), these parameters are defined as

$$\text{QE}, \lambda = \sum_{i=1}^{n} (l_1/l_0)^2/n \qquad (9)$$

and

$$\text{BAV}, \sigma = \sum_{i=1}^{n} (\theta_i - \theta_0)^2/(n-1). \qquad (10)$$

It is conventional to define l_0 and θ_0 as cation–anion bond lengths and anion–cation–anion bond angles in *regular* coordination polyhedra. However, in calculating the values in Tables 3 and 5, l_0 and θ_0 correspond to average values for the polyhedra concerned. This is thought to be more appropriate for AO_{12} cuboctahedra in tilted systems, where deviations from regularity are considerable.

Table 3 is divided essentially into two parts, with columns 3–7 referring to AO_{12} cuboctahedra and 8–12 to BO_6 octahedra. $QE^i(A)$ refers to the quadratic elongation of cation *A* with the cation at its experimentally determined position, whereas $QE^g(A)$ refers to the quadratic elongation which would arise if the ion were located at the geometrical centre of its coordination polyhedron. It is thus a measure of the distortion of the coordination polyhedron itself, independent of the position of the cation. Further, a value of $QE^i(A)$ greater than $QE^g(A)$ is indicative of a displacement of the *A* cation from the centre of its coordination polyhedron. The magnitude of this displacement is given in the column headed $dsp^i(A)$, with non-zero values obtained for all the structures in space group 62. Bond angle variances, calculated for angles in degrees, are typically greater than 100 for *A* ions in the structures, indicating significant deviations from a regular geometry. These characteristics are to be contrasted with those of the BO_6 octahedra, where the *B* ions are always located at the centres of their respective coordination octahedra. This is a consequence of the geometrical centres of the octahedra being located at positions of point symmetry $\bar{1}$ [Wyckoff position 4(*b*) in *Pnma*], whereby off-centre *B*-ion displacements and therefore dipole moments are precluded. It is to be noted that the octahedral distortions

Table 3. *Values of quadratic elongation, bond angle variance and magnitudes of cation displacements for structures in space group 62*

Composition	ICSD no.	$QE^i(A)$	$QE^g(A)$	$BAV^i(A)$	$BAV^g(A)$	$dsp^i(A)$ (Å)	$QE^i(B)$	$QE^g(B)$	$BAV^i(B)$	$BAV^g(B)$	$dsp^i(B)$ (Å)
$SrZrO_3$	500	1.01122	1.00988	103.632	104.580	0.1869	1.00001	1.00001	1.130	1.130	0.0000
$BaCeO_3$	2237	1.01057	1.00963	107.795	109.942	0.1705	1.00004	1.00004	1.834	1.834	0.0000
$BaPrO_3$	2239	1.00963	1.00826	111.197	110.557	0.2018	1.00000	1.00000	1.872	1.872	0.0000
$YAlO_3$	2526	1.02034	1.01562	113.840	105.024	0.3292	1.00002	1.00002	0.876	0.876	0.0000
$SmAlO_3$	4597	1.00865	1.00767	104.642	105.997	0.1465	1.00000	1.00000	0.467	0.467	0.0000
$NaTaO_3$	9090	1.00448	1.00488	142.360	139.636	0.1067	1.01232	1.01232	139.936	139.936	0.0000
$HoNiO_3$	10621	1.02433	1.01504	124.097	107.116	0.4302	1.00007	1.00007	6.237	6.237	0.0000
$PrFeO_3$	12457	1.01767	1.01435	109.111	105.465	0.2874	1.00001	1.00001	0.786	0.786	0.0000
$NdFeO_3$	12458	1.02024	1.01610	112.804	106.936	0.3227	1.00001	1.00001	0.872	0.872	0.0000
$SmFeO_3$	12459	1.02483	1.01922	118.779	107.998	0.3781	1.00004	1.00004	1.210	1.210	0.0000
$EuFeO_3$	12460	1.02685	1.02048	122.228	108.408	0.4042	1.00004	1.00004	1.592	1.592	0.0000
$TbFeO_3$	12462	1.03018	1.02286	127.989	110.621	0.4348	1.00005	1.00005	2.185	2.185	0.0000
$DyFeO_3$	12463	1.03202	1.02418	131.148	111.459	0.4516	1.00006	1.00006	2.338	2.338	0.0000
$HoFeO_3$	12464	1.03335	1.02512	133.917	112.715	0.4634	1.00005	1.00005	2.730	2.730	0.0000
$ErFeO_3$	12465	1.03484	1.02648	136.793	114.389	0.4713	1.00004	1.00004	2.684	2.684	0.0000
$TmFeO_3$	12466	1.03587	1.02719	138.501	115.623	0.4778	1.00003	1.00003	3.628	3.628	0.0000
$YbFeO_3$	12467	1.03762	1.02856	141.569	116.679	0.4898	1.00003	1.00003	3.881	3.881	0.0000
$LuFeO_3$	12468	1.03862	1.02948	143.922	119.039	0.4930	1.00003	1.00003	3.609	3.609	0.0000
$LaFeO_3$	13344	1.01168	1.01030	106.277	107.659	0.1843	1.00000	1.00000	0.882	0.882	0.0000
$KMnF_3$	15943	1.00504	1.00350	120.231	118.279	0.1494	1.00504	1.00350	20.774	20.774	0.0000
$KMnF_3$	15944	1.00622	1.00559	99.457	100.095	0.1216	1.00003	1.00003	6.073	6.073	0.0000
$KMnF_3$	15945	1.00361	1.00273	105.649	105.233	0.1494	1.00001	1.00001	0.566	0.566	0.0000
$GdFeO_3$	25957	1.02814	1.02106	135.771	123.091	0.4234	1.00070	1.00070	4.487	4.487	0.0000
$CaTiO_3$	26633	1.01337	1.01116	104.217	102.643	0.2283	1.01337	1.01116	0.375	0.375	0.0000
$CdTiO_3$	26634	1.02052	1.01765	110.326	107.955	0.2640	1.00000	1.00000	1.209	1.209	0.0000
$PrFeO_3$	27876	1.01854	1.01511	110.238	106.444	0.2950	1.00001	1.00001	0.564	0.564	0.0000
$SmNiO_3$	34154	1.01888	1.01482	114.716	108.929	0.3184	1.00002	1.00002	1.510	1.510	0.0000
$NaMgF_3$	36355	1.02027	1.01665	111.697	107.156	0.2964	1.00000	1.00000	1.134	1.134	0.0000
$NaNiF_3$	36356	1.02528	1.02021	118.789	109.722	0.3590	1.00000	1.00000	1.564	1.564	0.0000
$NaZnF_3$	36357	1.02645	1.02091	119.384	110.884	0.3725	1.00010	1.00010	2.947	2.947	0.0000
$NaCoF_3$	36358	1.02821	1.02284	122.308	112.817	0.3759	1.00000	1.00000	2.716	2.716	0.0000

inherent in the $NaTaO_3$ room-temperature structure are reflected by the values of $QE^i(B)$, $QE^g(B)$, $BAV^i(B)$ and $BAV^g(B)$ observed.

A similar treatment is given in Tables 4 and 5 for oxides and fluorides not in space group 62. In cases where there is more than one symmetry-independent AO_{12} and/or BO_6 polyhedron, $\Delta[V_A/V_B]$ values are referred to mean $[V_A/V_B]^a$ values. The magnitudes of $\Delta[V_A/V_B]$ are generally small, indicating good agreement between equation (8) and experimentally determined structures. The two obvious exceptions are $PbZrO_3$ (ICSD No. 15284) and $KCuF_3$, with $\Delta[V_A/V_B]$ values of -0.057 and -0.049, respectively. In the former case, the octahedra are very distorted, with $\Delta_{perp} = 9.649 \times 10^{-3}$. Furthermore, the octahedral stalks do not intersect, which is not reflected in the value of Δ_{perp}. It is to be noted that, in the most recent structural determination of $PbZrO_3$ (reference 25 in Table 1), the ZrO_6 octahedra are less distorted, with a lower $\Delta[V_A/V_B]$ value. However, the octahedral stalks still do not intersect one another. Unique to this structural solution is the assumption of disorder between two substructure components (Glazer, Roleder & Dec, 1993). The large magnitude of $\Delta[V_A/V_B]$ in $KCuF_3$ is due entirely to the significant deviation of the $(s_1 + s_s)^2/s_1s_2$ factor from 4.

It is seen in Table 5 that non-zero $dsp^i(B)$ values are allowed in many of the space groups, in contrast to space group 62 (see Table 3). Non-zero A-ion displacements are found in all space groups apart from 59, 127 and 140, although B-ion displacements can occur in the first of these.

(ii) *Hydrides of platinum or palladium with alkali ions*

Recent work concerning the synthesis and structures of some ternary platinum and palladium hydrides has revealed tilted perovskite-like structures, ABX_3, in which alkali metal *cations* (K^+, Rb^+, Cs^+) serve as X ions (as do the O^{2-} and F^- *anions* above), with hydride or deuteride *anions* acting as B ions and $[PdH_2]^{2-}$, $[PdH_4]^{2-}$ or $[PtH_4]^{2-}$ complex ions (or their deuteride equivalents) acting as A ions. Despite the rôle-reversal of cations and anions, the analysis can also be applied to these systems, as given in Tables 6 and 7.

Table 6 gives, in the main, the room-temperature crystallographic data for three classes of compound: (i) A_3PdD_3 ($A = K^+, Rb^+$); (ii) A_3PtD_5 ($A = K^+$, Rb^+, Cs^+); (iii) A_3PdD_5 ($A = Rb^+$). The predominant space group is no. 127 (*P4/mbm*), with $Z_{pc} = 4$, indicating that $\theta_z = 0$. A_3PdD_3 compounds, by comparison, crystallize in either space group 136 or 139, where $Z_{pc} = 8$. Agreement between $[V_A/V_B]^a$ and $[V_A/V_B]^t$ in Table 7 is excellent for the compounds in space group 127, good for K_3PdD_3 and Rb_3PdD_3 (room temperature) and rather poor for the cubic phase of Rb_3PdD_3 (at 473 K). The $\Delta[V_A/V_B]$ value of -0.092 is directly attributable to the large octahedral distortion, with $\Delta_{perp} = 1.508 \times 10^{-2}$.

Table 4. *Octahedral stalk lengths, tilt angles, polyhedral volumes and ratios, and values of Δ_{perp} for oxides and fluorides not in space group 62*

Composition	ICSD no.	s_1 (Å)	s_2 (Å)	s_3 (Å)	$(s_1+s_2)^2/s_1s_2$	θ_m (°)	θ_z (°)	V_A (Å^3)	V_B (Å^3)	$[V_A/V_B]^*$	$[V_A/V_B]^\dagger$	$\Delta[V_A/V_B]$	Δ_{perp}
$SrZrO_3$	1185	4.1621	4.1621	4.1475	4.000	6.345	0.000	58.9945	11.9744	4.927	4.927	0.000	0.000
$SrZrO_3$	1186	4.1728	4.1863	4.1400	4.000	8.847	2.605	58.1618	12.0481	4.827			3.802×10^{-4}
								58.8040		4.881			
								58.4829*		4.854*	4.852	−0.002	
$KMnF_3$	2471	4.1677	4.1677	4.1740	4.000	0.000	0.000	60.3661	12.0835	4.996	5.000	+0.004	0.000
		4.1853	4.1853	4.1740	4.000	5.256	0.000		12.1857	4.954	4.950		0.000
									12.1346*	4.975*	4.975*	0.000	
$KNbO_3$	3838	4.0344	4.0344	3.9710	4.000	0.000	0.000	53.8609	10.7722	5.000	5.000	0.000	1.120×10^{-5}
$NaNbO_3$	8460	3.9384	3.9384	3.9386	4.000	3.617	4.209	50.4631	10.1816	4.956	4.960	+0.004	7.098×10^{-6}
		3.9384	3.9384	3.9386	4.000	3.617	4.209	50.4638	10.1816	4.956			7.098×10^{-6}
								50.5389		4.964			
								50.5396		4.964			
								50.5014*	10.1816*	4.960*	4.960	0.000	
$NaNbO_3$	8461	3.9391	3.9392	3.9393	4.000	3.915	2.743	50.5782	10.1875	4.965			4.123×10^{-6}
								50.5796		4.965			
								50.5789*		4.965*	4.965	0.000	
$NaNbO_3$	9014	3.9638	3.9911	3.9307	4.000	10.199	9.213	49.0730	10.3637	4.735			1.882×10^{-5}
								49.1075		4.738			
								49.0903*		4.737*	4.737	0.000	
$NaTaO_3$	9091	3.9447	3.9463	3.9520	4.000	5.861	5.845	50.2867	10.2401	4.910			1.304×10^{-3}
								50.3521		4.917			
								50.3194*		4.914*	4.907	−0.007	
$NaTaO_3$	9092	3.9377	3.9453	3.9596	4.000	3.760	7.242	49.3181	10.2398	4.816			1.218×10^{-3}
								51.7225		5.051			
								50.5203*		4.934*	4.927	−0.007	
$NaTaO_3$	9093	3.9412	3.9412	3.9340	4.000	4.688	0.000	50.5135	10.1843	4.960	4.960	0.000	0.000
$NaNbO_3$	9094	3.9584	3.9586	3.9485	4.000	6.725	4.072	50.0602	10.3085	4.856			3.375×10^{-4}
								51.0597		4.953			
								50.5600*		4.905*	4.903	−0.002	
$NaNbO_3$	9325	3.9414	3.9414	3.9430	4.000	3.434	0.000	50.8249	10.2089	4.978	4.978	0.000	0.000
$PbZrO_3$	15284	4.1941	4.1941	4.1100	4.000	7.244	0.000	58.9762	11.9337	4.942			9.649×10^{-3}
		4.1941	4.1941	4.1100	4.000	7.244	0.000	59.4505		4.982			9.649×10^{-3}
								59.2134*		4.962*	4.905	−0.057	
$BaTiO_3$	15285	4.0132	4.0132	3.9900	4.000	0.000	0.000	53.5512	10.7102	5.000	5.000	0.000	2.624×10^{-6}
$CdTiO_3$	26635	3.9277	3.9291	3.9380	4.000	15.099	14.706	44.6566	10.1234	4.411	4.410	−0.001	5.331×10^{-4}
$KCuF_3$	31453	3.7704	4.5126	3.9245	4.032	0.000	0.000	56.1850	11.1289	5.049	5.000	−0.049	0.000
$PbZrO_3(a)$†		4.1804	4.2488	4.1898	4.000	8.409	10.985	57.0504	12.3706	4.612			2.580×10^{-3}
								60.9229		4.925			
								58.9867*		4.768*	4.764	−0.004	
$PbZrO_3(b)$†		4.1824	4.2407	4.1812	4.000	8.162	10.365	57.1384	12.3360	4.632			1.903×10^{-3}
								60.9073		4.937			
								59.0229*		4.785*	4.783	−0.002	

* Average value. † This structure is considered to be disordered, with two substructure components (*a*) and (*b*), each belonging to space group 55.

Three trends are observed in the V_A, V_B and V_A/V_B values: (i) values of V_B follow the expected variation with changing X ion (K^+, Rb^+, Cs^+): $V(DK_6)$ (values 27.2590 and 28.2334 Å^3) < $V(DRb_6)$ (values 31.0419, 31.8101, 32.0531 and 32.4697 Å^3) < $V(DCs_6)$ (36.6581 Å^3); (ii) values of V_A also follow the expected trend with varying X ion: $V([PdD_2]K_{12}) = 123.5100 < V([PdD_2]Rb_{12}) = 143.2054$; $V([PtD_4]K_{12}) = 131.0517 < V([PtD_4]Rb_{12}) = 147.7352 < V([PtD_4]Cs_{12}) = 169.3632$ Å^3; (iii) for a given X ion, values of V_A follow the trend $V(PdD_4^{2-}) > V(PtD_4^{2-}) > V(PdD_2^{2-})$, *e.g.* for $X = Rb^+$, these values are 149.6550 > 147.7352 > 143.2054 Å^3. It is also to be noted that the polyhedral volumes of mixed alkali metal compounds, K_2RbPtH_5 and K_2CsPtH_5 are consistent with trends (i) and (ii). The third trend is in agreement with the observation of Bronger & Auffermann (1992) that a relatively small increase in (unit cell) volume is to be found upon the substitution of $[PdH_4]^{2-}$ (or $[PdD_4]^{2-}$) for $[PdH_2]^{2-}$, consistent with a complex ion of formal composition $Pd^0(H^-)_2H_2$ rather than $Pd^{II}(H^-)_4$.

The phase transitions to be found upon increasing the temperature are also susceptible to the analysis. This behaviour is summarized in the column headed $T_{pc>c}$ in Table 6. Upon increasing the temperature, chemical decomposition occurs before a possible phase transition in three of the systems, Rb_3PdD_3 ($Im\bar{3}$ phase), K_3PtD_5 and Rb_3PdD_5. In the systems K_3PdD_3, Cs_3PtD_5 and Rb_3PtD_5, a transition to a cubic $Pm3m$ phase occurs at elevated temperatures, in which there is no octahedral tilting and therefore V_A/V_B is exactly equal to 5 (Thomas, 1989). In particular, $V_A = 5/6a^3_{cubic}$ and $V_B = 1/6a^3_{cubic}$, *i.e.*

$$V_{A,Pm3m}(K_3PdD_3) = 131.950 \text{ Å}^3;$$

$$V_{B,Pm3m}(K_3PdD_3) = 26.390 \text{ Å}^3;$$

$$V_{A,Pm3m}(Cs_3PtD_5) = 180.090 \text{ Å}^3;$$

Table 5. *Values of quadratic elongation, bond angle variance and magnitudes of cation displacements for structures not in space group 62*

Composition	ICSD no.	$QE^i(A)$	$QE^g(A)$	$BAV^i(A)$	$BAV^g(A)$	$dsp^i(A)$ (Å)	$QE^i(B)$	$QE^g(B)$	$BAV^i(B)$	$BAV^g(B)$	$dsp^i(B)$ (Å)
$SrZrO_3$	1185	1.00204	1.00204	2.390	2.390	0.0000	1.00000	1.00000	0.000	0.000	0.0000
$SrZrO^3$	1186	1.00543	1.00480	5.206	3.867	0.1048	1.00002	1.00002	0.908	0.908	0.0000
		1.00353	1.00352	6.292	5.960	0.0436					
$KMnF_3$	2471	1.00074	1.00070	0.935	0.815	0.0334	1.00000	1.00000	0.000	0.000	0.0000
							1.00000	1.00000	0.000	0.000	0.0000
$KNbO_3$	3838	1.00058	1.00002	2.423	0.192	0.1209	1.00364	1.00006	22.669	0.142	0.1998
$NaNbO_3$	8460	1.00143	1.00143	1.662	1.662	0.0000	1.00000	1.00000	0.017	0.017	0.0000
		1.00143	1.00143	1.597	1.597	0.0000	1.00000	1.00000	0.017	0.017	0.0000
		1.00081	1.00081	0.956	0.956	0.0000					
		1.00080	1.00080	0.890	0.890	0.0000					
$NaNbO_3$	8461	1.00136	1.00099	2.633	1.195	0.0944	1.00000	1.00000	0.010	0.010	0.0000
		1.00134	1.00098	2.473	1.062	0.0944					
$NaTaO_3$	9091	1.00296	1.00252	3.771	3.268	0.0665	1.00000	1.00000	3.115	3.115	0.0000
		1.00344	1.00272	10.336	3.334	0.1922					
$NaTaO_3$	9092	1.00310	1.00343	6.489	2.597	0.1564	1.00001	1.00001	2.908	2.908	0.0000
		1.00196	1.00203	8.981	2.610	0.1958					
$NaTaO_3$	9093	1.00112	1.00112	1.291	1.291	0.0000	1.00000	1.00000	0.000	0.000	0.0000
$NaNbO_3$	9014	1.00983	1.00786	17.461	8.749	0.2200	1.00162	1.00005	14.854	0.467	0.1482
		1.00746	1.00734	8.594	8.390	0.0385					
$NaNbO_3$	9094	1.00309	1.00281	4.659	3.372	0.0808	1.00000	1.00000	0.806	0.806	0.0000
		1.00267	1.00262	3.635	3.093	0.0493					
$NaNbO_3$	9325	1.00060	1.00060	0.693	0.693	0.0000	1.00000	1.00000	0.000	0.000	0.0000
$PbZrO_3$	15 284	1.01288	1.00529	38.973	27.167	0.3671	1.00243	1.00595	101.149	53.768	0.2099
		1.01386	1.00541	43.608	35.131	0.3671	1.00215	1.00641	94.962	45.077	0.2099
$BaTiO_3$	15 285	1.00014	1.00001	1.069	0.188	0.0682	1.00181	1.00005	7.692	0.084	0.1250
$CdTiO_3$	26 635	1.02047	1.01760	84.563	77.369	0.2642	1.02047	1.01760	1.582	1.848	0.0236
$KCuF_3$	31 453	1.00013	1.00013	8.053	8.053	0.0000	1.00618	1.00618	0.000	0.000	0.0000
$PbZrO_3(a)$*		1.01426	1.00712	25.097	16.984	0.3473	1.00053	1.00225	63.648	22.491	0.2130
		1.02083	1.01039	39.012	23.497	0.3844					
$PbZrO_3(b)$*		1.01435	1.00622	27.286	17.343	0.3771	1.00058	1.00266	68.959	26.181	0.2145
		1.02082	1.01155	38.999	24.864	0.3533					

*This structure is considered to be disordered, with two substructure components (*a*) and (*b*), each belonging to space group 55.

Table 6. *Crystal structural data of ternary platinum and palladium hydrides with perovskite-like structures*

Composition	*A*	*B*	*X*	Temperature (K)	Space group	Z_{pc}	a_{pc} (Å)	c_{pc} (Å)	γ_{pc} (°)	a_{cubic} (Å)	$T_{pc>c}$ (K)	Ref.
K_3PdD_3	$[PdD_2]^{2-}$	D^-	K^+	295	136	8	10.7000	10.535	90.0000	5.410	503	(1)
Rb_3PdD_3	$[PdD_2]^{2-}$	D^-	Rb^+	295	139	8	11.2150	11.083	90.0000		< 473*	(2)
Rb_3PdD_3	$[PdD_2]^{2-}$	D^-	Rb^+	473	204	8	11.305	11.305	90.0000		Decomp.	(2)
K_3PtD_5	$[PtD_4]^{2-}$	D^-	K^+	295	127	4	10.5670	5.706	90.0000		Decomp.	(3)
Cs_3PtD_5	$[PtD_4]^{2-}$	D^-	Cs^+	295	127	4	11.8044	5.914	90.0000	6.001	503	(3)
K_2RbPtH_5	$[PtH_4]^{2-}$	H^-	K^+, Rb^+	295	127	4	10.6844	5.808	90.0000		?	(3)
K_2CsPtH_5	$[PtH_4]^{2-}$	H^-	K^+, Cs^+	295	127	4	10.8513	5.949	90.0000		?	(3)
Rb_3PtD_5	$[PtD_4]^{2-}$	D^-	Rb^+	295	127	4	11.0705	5.868	90.0000	5.743	635	(3)
Rb_3PdD_5	$[PdD_4]^{2-}$	D^-	Rb^+	295	127	4	11.0309	5.987	90.0000		Decomp.	(2)

References: (1) Bronger & Auffermann (1990); (2) Bronger & Auffermann (1992); (3) Bronger, Auffermann & Müller (1988). * Phase transition to cubic $Im\bar{3}$ phase (T = 473 K structure), not to $Pm3m$ phase.

$$V_{B,Pm3m}(Cs_3PtD_5) = 36.018\ \text{Å}^3;$$

$$V_{A,Pm3m}(Rb_3PtD_5) = 157.847\ \text{Å}^3;$$

$$V_{B,Pm3m}(Rb_3PtD_5) = 31.569\ \text{Å}^3.$$

It is interesting to note that in each of these cases, V_A increases significantly in passing from the tetragonal to the cubic phase, whereas V_B falls slightly. The implication is that the vibrational and rotational modes of the $[PdD_2]^{2-}$ or $[PtD_4]^{2-}$ groups give rise to a stronger dependence of volume on temperature than for simple ions such as D^-, which occupy the *B* sites.

In the case of Rb_3PdD_3, a transition occurs to a cubic phase of $Im\bar{3}$ symmetry upon heating, with the structural characteristics as described in Tables 6 and 7 for the 473 K phase. Whereas there is essentially no change in $V_B(DRb_6)$ compared with the room-temperature phase, two of the eight AX_{12}, *i.e.* $[PdD_2]Rb_{12}$, polyhedra show a dramatic increase in polyhedral volume from 143.2 (average value) to 172.5 Å^3. The driving force for this phase transition is unclear, as is the significant increase in octahedral distortion in passing from the $I4/mmm$ to the $Im\bar{3}$ phase.

It is seen that the analysis provides a helpful framework for interpreting the structural variations amongst these novel chemical compounds.

(iii) *Evaluation of the proposed equation linking V_A/V_B with tilt angles θ_m and θ_z*

The foregoing analysis of Tables 1–7 supports the widespread applicability of equation (8), the closeness of agreement between $[V_A/V_B]^t$ and $[V_A/V_B]^a$ being dependent upon the degree of regularity of the octahedra. Two

Table 7. *Octahedral stalk lengths, tilt angles, polyhedral volumes and ratios and values of Δ_{perp} for structures in Table 6*

Composition	s_1 (Å)	s_2 (Å)	s_3 (Å)	θ_m (°)	θ_z (°)	V_A (Å^3)	V_B (Å^3)	$[V_A/V_B]^a$	$[V_A/V_B]^t$	$\Delta[V_A/V_B]$	Δ_{perp}
K_3PdD_3	5.4653	5.4653	5.4805	11.790	16.028	119.5980	27.2590	4.388			
						123.0396		4.514			
						125.7012		4.611			8.996×10^{-4}
						123.5100*		4.531*	4.526	−0.005	
Rb_3PdD_3 (295 K)	5.7035	5.7035	5.7034	10.527	14.752	139.8773	31.0419	4.506			
						141.3187		4.553			
						145.8127		4.697			8.461×10^{-4}
						143.2054*		4.613*	4.609	−0.004	
Rb_3PdD_3 (473 K)	5.7891	5.7891	5.7891	12.472	12.472	140.8871	31.8101	4.429			
						172.5047		5.423			
						148.7915*		4.677*	4.585	−0.092	1.508×10^{-2}
K_3PtD_5	5.4487	5.4487	5.7060	14.144	0.000	131.0517	28.2334	4.642	4.642	0.000	0.000
Cs_3PtD_5	6.0985	6.0985	5.9140	14.574	0.000	169.3632	36.6581	4.620	4.620	0.000	0.000
K_2RbPtH_5	5.5040	5.5040	5.8080	13.928	0.000	136.4296	29.3248	4.652	4.652	0.000	0.000
K_2CsPtH_5	5.6171	5.6171	5.9490	15.003	0.000	143.8399	31.2836	4.598	4.598	0.000	0.000
Rb_3PtD_5	5.7249	5.7249	5.8680	14.789	0.000	147.7352	32.0531	4.609	4.609	0.000	0.000
Rb_3PdD_5	5.7044	5.7044	5.9870	14.789	0.000	149.6550	32.4697	4.609	4.609	0.000	0.000

* Average value.

types of departure from regularity should be considered: (i) deviations of $(s_1 + s_2)^2/s_1s_2$ from 4 wherever $s_1 \neq s_2$ and (ii) departures of the angles of intersection of octahedral stalks form 90°, as expressed by the factor Δ_{perp}.

A concise and comprehensive overview of the relationship between V_A/V_B and octahedral tilting may be obtained by defining a parameter Φ to represent the degree of tilt, where

$$\Phi = 1 - \cos^2\theta_m \cos\theta_z. \quad (11)$$

This function has the essential attribute that it assumes the value of zero when there is no tilting, *i.e.* $\theta_m = \theta_z = 0$. Thus, the following linear relationship between V_A/V_B and Φ follows from (8)

$$V_A/V_B = 5 - 6\Phi. \quad (12)$$

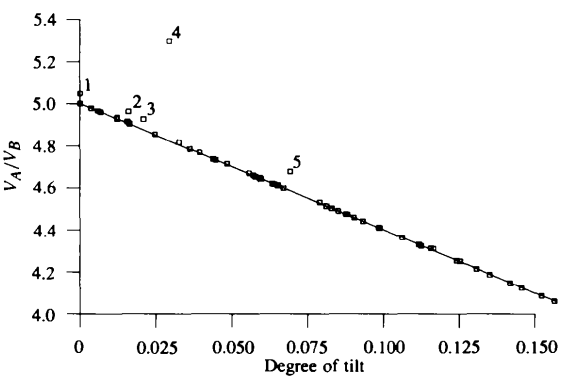

Fig. 2. Predicted variation of V_A/V_B with degree of tilt Φ as defined in equation (12). Experimental points are represented as small squares. In cases of significant deviation from the straight line, numbers indicate the structure responsible: (1) $KCuF_3$ (ICSD no. 31453), (2) $PbZrO_3$ (ICSD no. 15284), (3) $KMnF_3$ (ICSD no. 15943), (4) $NaTaO_3$ (ICSD no. 9090) and (5) Rb_3PdD_3 (473 K phase). Each of these is characterized by large octahedral distortions.

A plot of actual $[V_A/V_B]^a$ values *versus* degree of tilt Φ is given in Fig. 2. $[V_A/V_B]^a$ values are extracted from Tables 2, 4 and 7, and the corresponding Φ values calculated from the θ_m and θ_z values in these tables.

4. Discussion

4.1. *Relationship of this parameterization to Glazer's tilt system*

The system of analysis and nomenclature introduced by Glazer (1972) for tilting in perovskites permits an evaluation of the number and directions of tilts which are operative in a given structure. Thus, in a three-tilt system, tilting occurs about each of the pseudo-cubic x, y or z axes and in a two-tilt system about just two of these *etc.* Tilt directions are conveyed by a superscript +, − or 0. Thus, the notation $a^0b^-c^-$, for example, signifies zero tilt about the x axis and negative tilts about the y and z axes. Equality of tilts is denoted by repeated use of a particular axis symbol. For example, $a^0b^-b^-$ signifies that the tilts about the y and z axes are of equal magnitude and direction.

Insight into the structural significance of different tilt systems may be gained by consideration of Fig. 3, where single layers of octahedra in tilted structures are shown. The sign of a particular tilt is determined by the sequence of clockwise or anticlockwise rotations about the relevant axis. Thus, in Fig 3(a), by moving along the x axis in a positive direction, all the octahedra are tilted in the same sense (clockwise), giving rise to the notation a^+. By comparison, when moving along the positive y axis, the octahedra are rotated alternatively anticlockwise and clockwise, leading to the notation b^-. Note that only the a^-b^- (Fig. 3c), a^0b^- (not shown) and a^0a^0 (untilted; not shown) systems are consistent with the existence of a smaller orthorhombic unit cell. In all other cases, the pseudo-cubic cell itself is the unit cell.

Table 8. *Space group numbers, symbols, tilt systems, V_A/V_B values, A- and B-ion coordinations for the 13 space groups into which the structures analysed fall*

Space group no.	Space group symbol	Representative composition	ICSD no.	Tilt system	N_{tilt}	V_A/V_B	A-ion coordination	B-ion coordination
32	*Pba2*	$PbZrO_3$	15284	$a^0a^0c^+$	1	4.962	[4*i*, 4*i*, 3*i*, 1]	[1, 1, 1, 1, 1, 1]
33	*Pna2*$_1$	$CdTiO_3$	26635	$a^-a^-c^+$	3	4.411	[4*i*, 4*i*, 4*i*]	[3*i*, 3*i*]
38	*Amm2*	$BaTiO_3$	15285	$a^0a^0a^0$	0	5.000	[1, 4*r*, 2*r*, 4*r*, 1]	[2*r*, 2*r*, 2*r*]
55	*Pbam*	$PbZrO_3$	see Table 1	$a^-a^-c^+$	3	4.777	[4*i*, 4*i*, 4*i*] [3*i*, 1, 4*i*, 3*i*, 1]	[1, 1, 1, 1, 1, 1]
57	*Pbcm*	$NaNbO_3$	9014	$a^-a^-(c^+c^-c^+c^-)$	3	4.737	[3*i*, 6*i*, 3*i*] [1, 3*i*, 4*i*, 4*i*]	[1, 3*i*, 1, 1]
59	*Pmmn*	$NaNbO_3$	8460	$a^+b^-c^+$	3	4.960	[4*i*, 4*i*, 4*r*] [4*r*, 4*i*, 4*i*] [2*r*, 8*i*, 2*r*]	[6*i*]
62	*Pnma*	$YAlO_3$	2526	$a^-a^-c^+$	3	4.474	[4*i*, 4*i*, 4*i*]	[2*r*, 2*r*, 2*r*]
63	*Cmcm*	$NaTaO_3$	9092	$a^0b^-c^+$	2	4.934	[4*r*, 4*r*, 4*r*]	[2*r*, 2*r*, 2*r*]
127	*P4/mbm*	$NaNbO_3$	9325	$a^0a^0c^+$	1	4.971* 4.622†	[4*r*, 4*r*, 4*r*]	[6*i*]
136	*P4*$_2$*/mnm*	K_3PdD_3	see Table 6	$a^+a^+c^0$	2	4.531	[8*r*, 4*r*] [4*r*, 8*r*] [4*r*, 4*r*, 4*r*]	[6*i*]
139	*I4/mmm*	Rb_3PdD_3(rt)‡	see Table 6	$a^+a^+c^+$	3	4.613	[8*r*, 4*r*] [4*r*, 8*r*] [4*r*, 4*r*, 4*r*]	[6*i*]
140	*I4/mcm*	$SrZrO_3$	1185	$a^0a^0c^-$	1	4.927	[4*r*, 4*r*, 4*r*]	[6*i*]
204	*Im*$\bar{3}$	Rb_3PdD_3(ht)‡	see Table 6	$a^+a^+a^+$	3	4.677	[12*r*] [4*r*, 4*r*, 4*r*]	[6*r*]

* Average calculated for oxides and fluorides. † Average calculated for ternary platinum and palladium hydrides. ‡ rt = room temperature, ht = high temperature.

A second layer would be required, above the first, to determine possible tilt directions about the *z* axis. The requirement that the octahedra form a three-dimensional connected network limits the possible basic tilt systems to the following ten (Glazer, 1972): $a^+b^-c^-$ (derived from Fig. 3*a*); $a^+b^+c^+$, $a^+b^+c^-$ (derived from Fig. 3*b*); $a^-b^-c^-$ (derived from Fig. 3*c*); $a^0b^+c^+$, $a^0b^+c^-$ (derived from Fig. 3*d*); $a^0b^-c^-$ (derived from tilt system a^0b^-, not shown); $a^0a^0c^+$, $a^0a^0c^-$, $a^0a^0a^0$ (no tilting about the *x* and *y* axes).

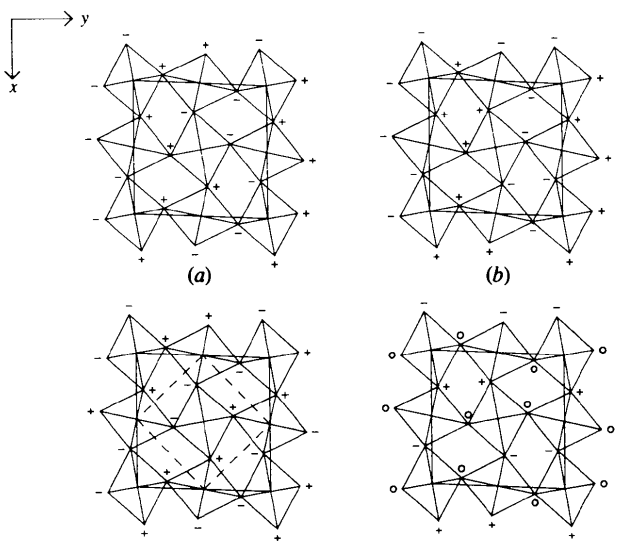

Fig. 3. Schematic representation of alternative tilt systems, as viewed in the *xy* projection referred to pseudo-cubic axes: (*a*) a^+b^-, (*b*) a^+b^+, (*c*) a^-b^- and (*d*) a^0b^+. Only the a^-b^- tilt system is consistent with a smaller orthorhombic cell, represented by the dashed line in (*c*).

The structures analysed here fall into 13 space groups, as given in Table 8, along with their associated tilt systems. The tilt analysis has been carried out computationally, by considering whether octahedral vertices lie above, below or in the pseudo-cubic planes *xy*, *yz* and *zx*. This approach is consistent with the notation used to denote the *z* height of octahedral vertices in Fig. 3.

It is to be noted that nine of the 13 space groups give rise to basic tilt systems of the type a^-b^-, a^0b^- or a^0a^0, which, apart from *Cmcm*, are consistent with the existence of a smaller orthorhombic unit cell. In the unique case of *Cmcm*, the C-centring also causes the pseudo-cubic cell to be the unit cell, with $a_{pc} \neq b_{pc}$ (see Table 1). The other four space groups also have the pseudo-cubic cell as their unit cell, of which three are associated with ternary hydrides of platinum and palladium. It may be inferred that the basic a^-b^- tilt sub-system (and derivatives a^0b^-, a^0a^0), and consequently the smaller, orthorhombic unit cell, are predominant amongst oxides and fluorides. The association of some tilt systems with more than one space group is attributable to variations in the distortions of coordination polyhedra and in cationic displacements.

Glazer's notation leads immediately to the number of tilt systems operative in a given structure (N_{tilt} in Table 8). This is not quite so straightforward from the definition of tilt angles, θ_m and θ_z, used here. However, the existence of a single-tilt system ($a^0a^0c^+$ or $a^0a^0c^-$) may be inferred directly from θ_z being equal to zero and a

Table 9. *Polyhedral volume ratios $\langle V_A/V_B\rangle$ averaged over structures in the different space groups, with corresponding values of N_{tilt}*

Sequence number	Space group	$\langle V_A/V_B\rangle$	N_{tilt}
1	38	5.000	0
2	140	4.988	1
3	127	4.971	1
4	32	4.962	1
5	59	4.960	3
6	63	4.914	2
7	55	4.777	3
8	57	4.737	3
9	204	4.677	3
10	139	4.613	3
11	136	4.531	2
12	62	4.475	3
13	33	4.411	3

zero-tilt system from both θ_z and θ_m being equal to zero. In order to discriminate between systems with two- and three-tilt systems, it is necessary to examine the *axes of rotation* to which angles θ_m and θ_z refer. As an example, the $NaNbO_3$ (8460) and $NaTaO_3$ (9092) structures are now considered. The first of these is a three-tilt system, $a^+b^-c^+$, and the second a two-tilt system, $a^0b^-c^+$. In $NaNbO_3$, θ_m angles refer to rotation axes [0, 0.82202, 0.56945] and [0.82202, 0, −0.56945], where the coordinates are fractional coordinates referred to pseudo-cubic axes. The θ_z angle refers to axis $[2^{1/2}/2, 2^{1/2}/2, 0]$. In the two-tilt $NaTaO_3$ structure, by comparison, θ_m angles refer to the rotation axis [0, −0.39683, −0.91789] with respect to the x axis and [0, 0, 1] with respect to the y axis. θ_z refers to the axis [0.02552, 0.99967, 0]. It is significant here that the axis for rotation with respect to the y axis is parallel to the z axis. This implies that there can be no tilting about the x axis, which is consistent with the operative tilt system, $a^0b^-c^+$.

For a full *derivation* of atomic coordinates from stalk lengths and θ_x, θ_y and θ_z tilt angles, it would also be necessary to know the rotation axes, as given above. Since these do not affect V_A/V_B, however, they have not been routinely quoted for the structures analysed.

4.2. *Trends in the observed tilt systems*

Consideration of Table 9 reveals that there is a correlation between the number of operative tilt systems, N_{tilt}, and mean polyhedral volume ratios, $\langle V_A/V_B\rangle$, with averages taken over all the structures analysed. As $\langle V_A/V_B\rangle$ falls, there is a general increase in N_{tilt}, with the exception of space groups 59 and 63 (sequence numbers 5 and 6) and space group 136. In the latter case, the assignation of tilt system should be regarded as provisional, as an R factor as high as 14% was quoted (Bronger & Auffermann, 1990). The authors noted that the 'structure of the low-temperature phase (of K_3PdD_3) should be refined by means of an extended data set of complementary neutron diffraction experiments'. It follows that, as the degree of tilt Φ increases, as defined by equation (12), the number of operative tilt systems also increases.

Information on coordination patterns of A and B ions in the different space groups is given in the two right-hand columns of Table 8. The notation refers to the distribution of $A—X$ and $B—X$ distances within the coordination polyhedra. For example, $[1, 4r, 2r, 4r, 1]$ indicates that there is one $A—X$ interaction of minimum length, a cluster of four interactions of equal, but longer length, followed by two of equal length, then four of equal length and finally a single interaction of maximum length. The notation 'i' and 'r' is used to denote whether the distances within a given cluster are equal (r, regular) or unequal, but close together (i, irregular). It is seen that essentially all $a^-a^-c^+$ systems have $[4i, 4i, 4i]$ AX_{12} polyhedra, but differences are observed in the BX_6 octahedra: space group 62 is the most regular, $[2r, 2r, 2r]$ and 55 the least regular [1, 1, 1, 1, 1, 1], with 33 of intermediate regularity, $[3i, 3i]$.

Polymorphic systems, such as $NaNbO_3$, are particularly informative, since a sequence of changes in tilt systems and AX_{12}/BX_6 geometries can be observed. The overall reduction in V_A/V_B from 5 in the $Pm3m$ cubic phase at 923 K to 4.702 in the 20 K rhombohedral phase is seen in Table 10. The room-temperature structure is of interest because of its complex tilt system. In this connection, the doubling of the pseudo-cubic c-parameter permits an alternation between c^+ and c^- in the z axis tilting. Also observed are two types of AO_{12} cuboctahedron as regards $A—O$ distances: $[3i, 6i, 3i]$ and $[1, 3i, 4i, 4i]$ (Table 8), with the first of these found in $a^-a^-c^-$ tilt regions and the second in $a^-a^-c^+$ regions. The first type of cuboctahedron is suggestive of rhombohedral symmetry (Thomas & Beitollahi, 1994), for which the appropriate tilt system is $a^-a^-a^-$ (Glazer, 1972). This is closely related to $a^-a^-c^-$. It is as if the room-temperature phase is an intergrowth, within each unit cell, of a pseudo-rhombohedral and an orthorhombic structure. Furthermore, it acts as a precursor to the $R3c$ rhombohedral phase which is formed at temperatures below 163 K (Darlington & Megaw, 1973; see Table 10).

It is also likely that the ternary platinum and palladium hydrides will be strongly polymorphic. This follows from the strong temperature dependence of V_A, owing to the vibrations and rotations of complex rather than simple ions. The expected wide variation in V_A/V_B will be associated with several different tilt systems. Thus, cooling A_3PtH_5 and A_3PdH_5 below room temperature is expected to lead to phases with $N_{tilt} > 1$ (*i.e.* lower V_A/V_B), as vibrations of the $[PdH_4]^{2-}$ and $[PtH_4]^{2-}$ complex ions 'freeze out'.

4.3. *Treatment of rhombohedral perovskites*

It has been shown recently (Thomas & Beitollahi, 1994) that the relationship between polyhedral volume

Table 10. *Temperatures, space groups, tilt systems, polyhedral volumes and B-ion displacements in the $NaNbO_3$ system*

Temperature (K)	ICSD no./ reference	Space group symbol	Tilt system	N_{tilt}	V_A (Å^3)	V_B (Å^3)	V_A/V_B	dsp^t (B)
923	(1)	*Pm3m*	$a^0a^0a^0$	0	50.748	10.150	5.000	0.0
873	9325	*P4/mbm*	$a^0a^0c^+$	1	50.825	10.209	4.978	0.0
813	9094	*Cmcm*	$a^0b^-c^+$	2	50.560	10.309	4.905	0.0
803	8461	*Cmcm*	$a^0b^-c^+$	2	50.579	10.188	4.965	0.0
773	8460	*Pmmn*	$a^+b^-c^+$	3	50.501	10.182	4.960	0.0
295	9014	*Pbcm*	$a^-a^-(c^+c^-)$	3	49.090	10.364	4.737	0.1482
123	13 245	*R3c*	$a^-a^-a^-$	3	49.284	10.407	4.735	0.2721
20	(2)	*R3c*	$a^-a^-a^-$	3	49.183	10.460	4.702	0.2426

References: (1) Thomas (1989); (2) (in CODEN form) ZEKGA 143 44 1976.

Table 11. *Rhombohedral perovskites: space groups, pseudo-cubic cell parameters and tilt angles; rhombohedral tilt angles and pseudo-cubic tilt angles calculated from equation (14). Comparison of actual V_A/V_B ratio with values calculated from equations (13) and (8)*

Composition	Temperature (K)	Space group no.	a_{PC} (Å)	α_{PC} (°)	θ_{PC} (°)	$\langle\omega\rangle_r$ (°)	θ_{PC}^{calc} (°)	$[V_A/V_B]^a$	$[V_A/V_B]^r$	$[V_A/V_B]^{PC}$	ICSD no.
$KNbO_3$	230	160	8.0320	89.8170	0.000	0.000	0.000	5.000	5.000	5.000	3839
$LiNbO_3$	293	161	7.5293	86.2723	18.733	23.262	19.083	4.065	4.064	4.096	17 292
$PrAlO_3$	293	166	7.5240	90.2848	0.000	0.000	0.000	5.000	5.000	5.000	17 790
$LaCoO_3$	293	167	7.6516	90.6856	8.049	9.769	7.983	4.827	4.827	4.824	25 292

ratio, V_A/V_B, and mean octahedral tilt angle in rhombohedral perovskites, $\langle\omega\rangle_r$, corresponds to

$$V_A/V_B = 6K^2\cos^2\langle\omega\rangle_r - 1, \qquad (13)$$

where $K \simeq 1$ and ω is the angle of octahedral rotation about the trigonal axis. Since all perovskite structures can be defined in pseudo-cubic axes, it follows that the tilting in rhombohedral systems can also be quantified in terms of tilt angles θ_m and θ_z, as defined in equation (8) and the preceding derivation. By comparison with orthorhombic and tetragonal perovskites, the derived pseudo-cubic axes for rhombohedral structures have no unique z axis, *i.e.* $\theta_z = \theta_m$. If this common angle is denoted as θ_{PC}, a comparison of equations (8) and (13) leads to the result

$$\theta_{PC} = \cos^{-1}\{\cos^{2/3}\langle\omega\rangle_r\}. \qquad (14)$$

The applicability of this result is investigated in Table 11 for four structures, one from each of the rhombohedral space groups *R3m* (no. 160), *R3c* (no. 161), *R$\bar{3}$m* (no. 166) and *R$\bar{3}$c* (no.167). a_{PC} and α_{PC} are the parameters of the derived pseudo-cubic cell, which is also rhombohedral. θ_{PC} is the measured tilt angle for the structures, *i.e.* the angle subtended by octahedral stalks with their nearest pseudo-cubic axes; $\langle\omega\rangle_r$ is the rhombohedral tilt angle (Thomas & Beitollahi, 1994) and θ_{PC}^{calc} the value of θ_{PC} calculated from (14). For non-zero θ_{PC} values ($LiNbO_3$ and $LaCoO_3$), it is seen that the agreement between θ_{PC} and θ_{PC}^{calc} is only approximate. Furthermore, the value of V_A/V_B calculated from (13), $[V_A/V_B]^r$, is considerably more accurate than the value calculated from (8), $[V_A/V_B]_{PC}$. Therefore, it is always advisable to use the parameterization developed explicitly for rhombohedral perovskites, based on (13).

The reasons for the discrepancies between calculated and experimental pseudo-cubic tilt angles and V_A/V_B ratios are straightforward. First, the pseudo-cubic z axis is no longer perpendicular to the xy plane, as was assumed in the derivation of (9) for orthorhombic and tetragonal systems, and γ_{PC} is always different from 90°. A correction for this would lead to the result

$$V_A/V_B \simeq 6\cos^2\theta_m\cos\theta_z\sin\alpha_{pc} - 1. \qquad (15)$$

The $\sin\alpha_{pc}$ correction factor is equal to 0.9979 for $LiNbO_3$, leading to a corrected $[V_a/V_b]_{pc}$ value of 4.085, in closer agreement with the experimental value. The second source of the discrepancy results from the assumption that the stalks of the octahedra intersect at right angles to one other. This is not generally the case. In connection with the octahedral distortions to be found in rhombohedral perovskites, the parameterization developed previously (Thomas & Beitollahi, 1994) is again superior, with just one parameter, Δs, required.

4.4. *Structural requirements for ferroelectricity and antiferroelectricity; inter-relationship of octahedral and rhombohedral symmetry*

The vast majority of structures analysed are neither ferroelectric nor antiferroelectric. Since ferroelectric materials necessarily belong to a polar space group, the only candidates for ferroelectric properties are $PbZrO_3$ (ICSD no. 15284), $CdTiO_3$ (ICSD no. 26635), $BaTiO_3$ (ICSD no. 15285) and $KNbO_3$ (ICSD no. 3838). Of these, $BaTiO_3$ and $KNbO_3$ are well known ferroelectrics. However, the degree of tilt in these systems is zero. The question arises as to whether ferroelectricity occurs in tilted systems of orthorhombic symmetry such as $PbZrO_3$ and $CdTiO_3$. In the first case, the dielectric behaviour is

known to correspond to that of an antiferroelectric. Moreover, the latest structural determination of $PbZrO_3$ has suggested a disordered structure with two substructure components, each of *non-polar* symmetry *Pbam*, as quoted in Tables 1, 4 and 5. In the latter case, the proposed structure ($Pna2_1$; ICSD no 26635) was investigated only as an alternative to the centrosymmetric *Pnma* structure [ICSD No. 26634 (Sasaki, Prewitt, Bass & Schulze, 1987)]. The authors concluded, on the grounds of their structural determination and the lack of observable ferroelectric behaviour, that the room-temperature structure of $CdTiO_3$ could be better described in *Pnma*.

The conclusion to be drawn is that whereas tilted orthorhombic and tetragonal perovskites have the capability of showing ferroelectric properties, by means of appropriate cationic displacements, no system has been found to date in which this capability has been exploited. It follows that the most promising way of obtaining ferroelectric properties in a *tilted* system is through a perovskite of rhombohedral *R3c* symmetry (tilt system $a^-a^-a^-$), where the symmetry dictates that any octahedral distortions give rise to *parallel* *B*-ion displacements (Thomas & Beitollahi, 1994). In the paper of Thomas & Beitollahi (1994), several systems in space group *R3c* were identified, thereby showing ferroelectric properties, including $NaNbO_3$ at 123 K and $LiNbO_3$, over a wide temperature range from room temperature up to 1483 K, its Curie point.

Consideration of $NaNbO_3$ in Table 10 shows that V_B adopts its maximum values in the two rhombohedral structures, although these are at the lowest temperatures. These large volumes are also associated with maximum *B*-ion displacements from the centres of their octahedra. Upon heating from 20 K to room temperature, at which an orthorhombic phase is stabilized, it is seen that V_B falls, as does $dsp^i(B)$. In the room-temperature phase, the NbO_6 octahedra give rise to electric dipoles, but the parallel alignment is lost, giving rise to antiferroelectric behaviour. In all the phases at higher temperatures, $dsp^i(B)$ is equal to zero, which is consistent with their paraelectric behaviour. It appears also that the *B*-ion octahedral volume V_B can be correlated with the existence or otherwise of a BO_6 dipole moment: when $V(NbO_6)$ takes on a value equal to 10.364 Å^3 or greater, the niobium ion is stabilized at an off-centre position.

Although tantalum is chemically and geometrically similar to niobium, $NaTaO_3$ does not give rise to antiferroelectric properties, even though the tilt sequence is analogous to that of $NaNbO_3$: [ICSD no. 9090; room temperature; space group 62; $a^-a^-c^+$]$\longrightarrow$[ICSD no. 9091; 803 K; space group 63; $a^0b^-c^+$]$\longrightarrow$[ICSD no. 9092; 873 K; space group 63; $a^0b^-c^+$]$\longrightarrow$[ICSD no. 9093; 893 K; space group 127; $a^0b^0c^+$]. In all cases, the Ta^{5+} ions are constrained to lie at the centres of their coordination octahedra, since they occupy special positions of symmetry $\bar{1}$, $\bar{1}$ and $4/m$ in space groups 62, 63 and 127, respectively. In this connection, a correlation between V_B and $dsp^i(B)$ is again found. V_B values in orthorhombic perovskites range between 10.184 and 10.240 Å^3, less than the value of 10.374 Å^3 in ferroelectric $LiTaO_3$, in which an off-centre displacement of 0.2017 Å is found (Thomas & Beitollahi, 1994).

Table 12. *Summary of polyhedral volumes, A-ion displacements and radii (Shannon, 1976) in orthorhombic and rhombohedral aluminates*

Composition	Space group symbol	V_A (Å^3)	V_B (Å^3)	V_A/V_B	$dsp^i(A)$	$r^{VI}(A)$
$YAlO_3$	*Pnma*	41.605	9.300	4.474	0.3292	0.900
$SmAlO_3$	*Pnma*	43.176	9.122	4.733	0.1465	0.958
$NdAlO_3$	$R\bar{3}c$	43.721	9.082	4.814	0.0000	0.983
$PrAlO_3$	$R\bar{3}m$*	44.366	8.873	5.000	0.0000	0.99

* $R\bar{3}c$ symmetry changes to $R\bar{3}m$ in the absence of tilting ($V_A/V_B = 5$).

In general, the factors governing whether rhombohedral or orthorhombic structures are preferentially stabilized are far from clear, although the issue is of great importance in obtaining ferroelectric behaviour in systems with tilted octahedra. In $LiNbO_3$, for example, the *A* ion (*i.e.* Li^+) is also instrumental in stabilizing the rhombohedral phase up to 1483 K. In $NaNbO_3$, the Na^+ ion is less effective in this regard, with a transition to orthorhombic symmetry at 163 K. The issue also arises in connection with non-polar tilted rhombohedral structures, which crystallize in space group 167 ($R\bar{3}c$): what governs whether a particualr structure crystallizes in $R\bar{3}c$ or in orthorhombic *Pnma*? A clue is to be found in that both *A*- and *B*-ion off-centre displacements are constrained to be zero in $R\bar{3}c$, whereas in *Pnma*, *A*-ion displacements are permitted. This feature is immediately apparent in a consideration of the four aluminates, $YAlO_3$, $SmAlO_3$ (Tables 2 and 3), $NdAlO_3$ and $PrAlO_3$ (Thomas & Beitollahi, 1994), as summarized in Table 12. By using the ionic radius in sixfold coordination as the criterion for ionic size (Shannon, 1976), it is seen that the larger ions Nd^{3+} and Pr^{3+} give rise to rhombohedral symmetry, with the structures consisting of smaller *A* ions crystallizing in *Pnma*. In this orthorhombic space group, the smaller ions are able to adopt larger coordination polyhedra, merely by off-centre displacements as a compensation. This is seen in the case of $SmAlO_3$, where, although the ionic radius of Sm^{3+} is less than that of Nd^{3+}, the V_A cuboctahedral volumes are comparable. The energetic advantage to be gained from adopting a larger AO_{12} polyhedron lies in a reduction of oxygen-ion repulsive energy.

Note that off-centre *A*-ion displacements are also possible within rhombohedral symmetry, but only within the *polar* space group *R3c*. Such an option would give rise to a net dipole moment, with consequences for electrostatic energy, which would not arise in non-polar *Pnma*. An intuitive understanding of the widespread adoption of *Pnma* in tilted perovskites may be stated as follows. The *B*-ion tends to adopt an octahedral volume

consistent with its ionic radius, whereby the centrosymmetric symmetry of the BO_6 octahedron prohibits off-centre displacement. The A ion adopts a V_A volume larger than would be suggested from its ionic radius, in order to minimize oxygen-ion repulsions within the coordination polyhedron. As a consequence, the degree of tilt is also reduced. It is able to fulfil its bonding requirements, however, by an off-centre displacement within the O_{12} polyhedron, in order to achieve closer coordination by oxygen ions.

Examination of Table 3 confirms that significant $dsp^i(A)$ values are found for all compositions. Amongst the ternary iron oxides, for example, the largest displacement, 0.4930 Å, occurs in $LuFeO_3$, with the smallest in $LaFeO_3$, 0.1843 Å. This reflects that Lu^{3+} has the smallest ionic radius amongst these compounds and La^{3+} the highest [$r^{VI}(Lu^{3+}) = 0.861$; $r^{VI}(La^{3+}) = 1.032$ Å (Shannon, 1976)]: smaller ions require larger displacements in order to optimize their coordination by oxygen ions. Although there is a parallel reduction in V_A in proceeding in from $LaFeO_3$ to $LuFeO_3$, A-ion displacement is an important complementary mechanism for stabilizing smaller A ions in the *Pnma* space group.

The question of orthorhombic *versus* rhombohedral symmetry in tilted perovskites is an important issue in the current generation of ceramic fuel cells, in which perovskites frequently function as cathodes and interconnect in a composite structure. The symmetry has a direct bearing on interfacial bonding between components of the composite and on the compatibility of their thermal expansion coefficients. A common interconnect material is based on $LaCrO_3$, which is orthorhombic at room temperature, but undergoes a transition to rhombohedral symmetry at 553 K. It has been found that doping $LaCrO_3$ with Sr^{2+} stabilizes the rhombohedral phase at room temperature, whereas doping with Ca^{2+} stabilizes the orthorhombic phase to temperatures higher than 553 K (Minh, 1993). This trend is consistent with the behaviour of the aluminates, which has been rationalized above. Ca^{2+}, being a smaller ion than the parent La^{3+} ion, promotes the A-ion displacements associated with orthorhombic *Pnma* symmetry, whereas Sr^{2+}, which is larger than La^{3+}, reduces the tendency towards A-ion displacement, thereby promoting rhombohedral symmetry.

The fine energy balances between orthorhombic and rhombohedral symmetry in many compositions are worthy of experimental investigation, since they will provide structural data upon which a more complete understanding can be built. By varying the temperatures at which structural determinations are carried out, it is envisaged that the inherent polymorphism of these tilted systems can be revealed and analysed. The achievement of ferroelectric properties through the adoption of the polar space group $R3c$ is also a likelihood, since systems with small A ions have an intrinsic tendency towards ionic displacements.

Table 13. *Summary of minimum and maximum AO_{12} and BO_6 polyhedral volumes observed in oxide perovskites at room temperature*

A ion	$V_{A,min}$ (Å^3)	$V_{A,max}$ (Å^3)	B ion	$V_{B,min}$ (Å^3)	$V_{B,max}$ (Å^3)
Ba^{2+}	53.373	70.031	Al^{3+}	8.873	9.300
Bi^{3+}	51.587	51.587	Ce^{4+}	14.995	14.995
Ca^{2+}	45.965	46.301	Co^{3+}	9.607	9.607
Cd^{2+}	44.654	44.657	Fe^{3+}	10.760	10.913
Dy^{3+}	45.716	45.716	Nb^{5+}	10.364	10.785
Eu^{3+}	46.992	46.992	Ni^{3+}	9.681	9.962
Er^{3+}	44.920	44.920	Pr^{4+}	14.657	14.657
Gd^{3+}	46.717	46.717	Re^{5+}	9.661	9.661
Hg^{2+}	46.506	46.506	Ta^{5+}	9.365	10.374
Ho^{3+}	43.310	45.270	Ti^{4+}	9.496	10.726
K^+	53.861	53.927	U^{5+}	12.475	12.475
La^{3+}	46.377	49.995	Zr^{4+}	11.934	12.371
Li^+	40.499	51.032			
Lu^{3+}	43.881	43.881			
Na^+	49.090	49.638			
Nd^{3+}	43.719	48.300			
Pb^{2+}	52.813	59.131			
Pr^{3+}	44.366	48.809			
Sm^{3+}	43.176	47.398			
Sr^{2+}	49.585	56.759			
Tb^{3+}	46.109	46.109			
Tm^{3+}	44.684	44.684			
Y^{3+}	41.605	41.605			
Yb^{3+}	44.214	44.214			

4.5. *Definition of transferable polyhedral volume ranges; prediction of degree of tilt from chemical composition; strategies for developing new ferroelectric compositions*

The analysis of perovskites, as carried out here and in preceding articles (Thomas, 1989; Thomas & Beitollahi, 1994), has employed experimentally determined structural data as the starting point. In so doing, a body of data has been built up concerning the A and B polyhedral volumes adopted by cations in perovskites, which is transferable to novel hypothetical perovskite systems. This information is summarized in Table 13, which gives the minimum and maximum AO_{12} and BO_6 volumes observed in room-temperature structures. V_A and V_B values calculated in the two previous articles have also been used in compiling the table.

By combining A and B ions of total valence equal to six, a hypothetical composition may be formed, *e.g.* K^+ and U^{5+} form KUO_6, for which V_A/V_B would lie between these limits: $53.861/12.475 < V_A/V_B < 53.927/12.475$, *i.e.* $4.318 < V_A/V_B < 4.323$. Application of equation (12) predicts a degree of tilt Φ in the range $0.1137 > \Phi > 0.1128$, which can be translated either into a rhombohedral tilt angle, $19.70 > \langle\omega\rangle_r > 19.63°$, or into a mean orthorhombic tilt angle ($\theta_{mean} = \theta_m = \theta_z$) of $16.142 > \theta > 16.079°$. No attempt will be made here to speculate whether rhombohedral or orthorhombic symmetry would be adopted, nor, in the former case, whether the polar space group $R3c$ would be found, this being a necessary condition for ferroelectric properties to arise.

In applying this technique, it should be borne in mind that there are limits of stability for the perovskite phase,

which may be expressed in terms of an allowed range of V_A/V_B values. The minimum observed V_A/V_B ratio observed to date corresponds to 4.060, this value being empirically determined from the structure $LuFeO_3$. It is essentially oxygen-ion repulsions which impose a lower limit on V_A/V_B. The upper limit to V_A/V_B, which is found in the absence of tilting, is equal to 5. Although exceptions to this upper limit arise in the $NaTaO_3$ (ICSD no. 9090) and $KCuF_3$ structures, this is at the expense of considerable octahedral distortion, which must be regarded as atypical. The usual consequence of the upper limit being exceeded is the adoption of an alternative structural type involving face-sharing octahedra (Thomas, 1991*b*).

In searching for new ferroelectric systems, it is probably most effective to investigate hypothetical compositions with predicted V_A/V_B ratios close to the upper limit of 5, particularly those with a *hypothetical* ratio slightly higher than 5. Thus, adoption of an *actual* ratio of 5 would be achieved by expansion of the BO_6 octahedron, a feature conducive to off-centre *B*-ion displacements. Any such structure would also be characterized by the absence of octahedral tilting, thereby reducing the possibility of polymorphism between (not necessarily ferroelectric) rhombohedral and (non-ferroelectric) orthorhombic phases. From Table 13, it may be deduced that the well known ferroelectric $BaTiO_3$ would have a hypothetical V_A/V_B ratio of between 4.976 and 7.375, the broad range indicating the wide variation in V_A volumes associated with the Ba^{2+} ion. In adopting the actual V_A/V_B ratio of 5 in ferroelectric $BaTiO_3$, it follows that the barium ion is tightly coordinated and the titanium ion loosely co-ordinated. Herein lies the driving force for displacements of the Ti^{4+} ion.

Formation of simple perovskite compositions is often limited by the valences of the *A* and *B* ions, necessitating the use of complex perovskites. For example, a likely ferroelectric composition containing the Fe^{3+} ion would require a minimum V_A volume of $5 \times 10.913 = 54.565$ Å^3. Only the Ba^{2+}, K^+ and Pb^{2+} ions are possible candidates here, although none have the required valence of three. By forming a complex perovskite, a ferroelectric composition may be postulated, *e.g.* $Pb(Fe^{3+}_{0.5}Nb^{5+}_{0.5})O_3$. This composition is known to show ferroelectric properties (Stenger & Burggraaf, 1980). The influence of mixed *B*-site ions on crystal symmetry is also worthy of further investigation. In this context, it is likely that the system $Pb(Zr_xTi_{1-x})O_3$ ($0.52 < x < 0.93$) is stabilized in rhombohedral symmetry (*R*3*m* and *R*3*c*) by the presence of both Zr^{4+} and Ti^{4+} ions on *B* sites (Thomas & Beitollahi, 1994). Also worthy of investigation is the extent to which certain ions promote off-centre displacements more than others, on the grounds of their electronic structures.

The analysis of octahedral tilting developed here may also be applied to layered and slab-like perovskite-related structures, such as the Aurivillius compounds. Recent crystallographic data have been published on the ferroelectric phases of Bi_3TiNbO_9 (Thompson, Rae, Withers & Craig, 1991) and $Bi_4Ti_3O_{12}$ (Rae, Thompson, Withers & Willis, 1990). Both of these show octahedral tilting, which can be analysed in terms of equation (8). Significant octahedral tilting is also to be found in the slab-like perovskite $Sr_2Nb_2O_7$ (Ishizawa, Marumo, Kawamura & Kimura, 1975). Each of these compositions has potential applications as a high-temperature ferroelectric or piezoelectric, by virtue of their high Curie points, T_c: 948 K in $Bi_4Ti_3O_{12}$, 1213 K in Bi_3TiNbO_9 and 1613 K in $Sr_2Nb_2O_7$. In each of these compositions the tilted octahedral configuration is imposed by the layered structure and it is stable at all temperatures up to the Curie point. Furthermore, the tilted structures act to *stabilize* the off-centre cationic displacements responsible for ferroelectricity. Such a stabilizing function is not found in the perovskite structures which have been analysed here.

It has been demonstrated in this article that an approach based on the calculation of polyhedral volumes provides a quantitative framework for understanding the dependence of all perovskite crystal structures on chemical composition. By virtue of its universal applicability, it is hoped that the methodology will act as a stimulus to further work in the various areas of research into perovskites, whether physical, chemical or mineralogical in emphasis.

Acknowledgement is made of the use of the EPSRC-funded Chemical Databank Service for part of the work.

References

Bronger, W. & Auffermann, G. (1990). *J. Less-Common Met.* **158**, 163–167.

Bronger, W. & Auffermann, G. (1992). *J. Alloys Compd.* **179**, 235–240.

Bronger, W., Auffermann, G. & Müller, P. (1988). *Z. Anorg. Allg. Chem.* **566**, 31–38.

Darlington, C. N. W. & Megaw, H. D. (1973). *Acta Cryst.* B**29**, 2171–2185.

Glazer, A. M. (1972). *Acta Cryst.* B**28**, 3384–3392.

Glazer, A. M. (1975). *Acta Cryst.* A**31**, 756–762.

Glazer, A. M., Roleder, K. & Dec, J. (1993). *Acta Cryst.* B**49**, 846–852.

Ishizawa, N., Marumo, T., Kawamura, T. & Kimura, M. (1975). *Acta Cryst.* B**31**, 1912–1915.

Megaw, H. D. (1966). *Proceedings of the International Meeting on Ferroelectricity*, Prague, Vol. 1, pp. 314–321.

Megaw, H. D. (1969). *Proceedings of the European Meeting on Ferroelectricity*, Saarbrücken, pp. 27–35.

Minh, N. Q. (1993). *J. Am. Ceram. Soc.* **76**, 563–588.

Rae, A. D., Thompson, J. G., Withers, R. L. & Willis, A. C. (1990). *Acta Cryst.* B**46**, 474–487.

Robinson, K., Gibbs, G. V. & Ribbe, P. H. (1971). *Science*, **172**, 567–570.

Sasaki, S., Prewitt, C. T., Bass, J. D. & Schulze, W. A. (1987). *Acta Cryst.* C**43**, 1669–1674.
Shannon, R. D. (1976). *Acta Cryst.* A**32**, 751–767.
Stenger, C. G. F. & Burggraaf, A. J. (1980). *Phys. Status Solidi A*, **61**, 653–662.
Thomas, N. W. (1989). *Acta Cryst.* B**45**, 337–345.
Thomas, N. W. (1991*a*). *Acta Cryst.* B**47**, 180–191.
Thomas, N. W. (1991*b*). *Acta Cryst.* B**47**, 597–608.
Thomas, N. W. & Beitollahi, A. (1994). *Acta Cryst.* B**50**, 549–560.
Thompson, J. G., Rae, A. D., Withers, R. L. & Craig, D. C. (1991). *Acta Cryst.* B**47**, 174–180.